Analytica Chimica Acta 936 (2016) 229–235

Contents lists available at ScienceDirect

Analytica Chimica Acta

journal homepage: www.elsevier.com/locate/aca

# Chemiluminescence imaging for microRNA detection based on cascade exponential isothermal amplification machinery

Yongjie Xu [a], Dandan Li [a], Wei Cheng [c], Rong Hu [a], Ye Sang [a], Yibing Yin [a], Shijia Ding [a, *], Huangxian Ju [a, b, *]

[a] Key Laboratory of Clinical Laboratory Diagnostics (Ministry of Education), College of Laboratory Medicine, Chongqing Medical University, Chongqing 400016, China
[b] State Key Laboratory of Analytical Chemistry for Life Science, Department of Chemistry, Nanjing University, Nanjing 210023, China
[c] The Center for Clinical Molecular Medical Detection, The First Affiliated Hospital of Chongqing Medical University, Chongqing 400016, China

## HIGHLIGHTS

- A new chemiluminescence imaging method for miRNA assay was developed based on cascade EXPAR strategy.
- The imaging method achieved ultrasensitivity and good specificity.
- The biosensing method possessed the merits of isothermal and homogeneous assay system.

## GRAPHICAL ABSTRACT

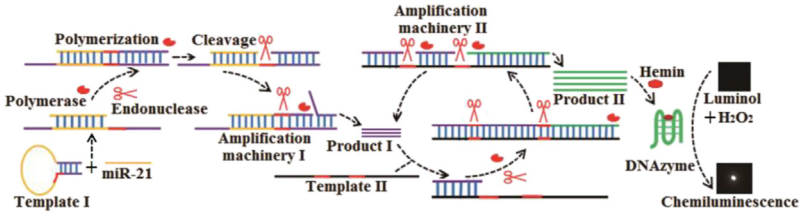


## ARTICLE INFO

*Article history:*
Received 21 March 2016
Received in revised form
29 June 2016
Accepted 5 July 2016
Available online 8 July 2016

*Keywords:*
Chemiluminescence imaging
MicroRNA
Exponential isothermal amplification reaction
Horseradish peroxidase-mimicking DNAzyme

## ABSTRACT

A novel G-quadruplex DNAzyme-driven chemiluminescence (CL) imaging method was developed for ultrasensitive and specific detection of miRNA based on the cascade exponential isothermal amplification reaction (EXPAR) machinery. A structurally tailored hairpin probe switch was designed to selectively recognise miRNA and form hybridisation products to trigger polymerase and nicking enzyme machinery, resulting in the generation of product I, which was complementary to a region of the functional linear template. Then, the response of the functional linear template to the generated product I further activated the exponential isothermal amplification machinery, leading to synthesis of numerous horseradish peroxidase mimicking DNAzyme units for CL signal transduction. The amplification paradigm generated a linear response from 10 fM to 100 pM, with a low detection limit of 2.91 fM, and enabled discrimination of target miRNA from a single-base mismatched target. The developed biosensing platform demonstrated the advantages of isothermal, homogeneous, visual detection for miRNA assays, offering a promising tool for clinical diagnosis.



## 1. Introduction

MicroRNAs (miRNAs) are small endogenous non-coding RNAs (18–25 bases) that function as part of the gene expression regulating machinery at the transcriptional and post-transcriptional levels [1,2]. Recent progresses in miRNA research has revealed that miRNAs are critical components of various pathophysiological processes [3] and that abnormal expression of miRNAs is associated with many human diseases [4]. For example, overexpression of some miRNAs, termed oncomiRs, plays a key role in the onset and progression of cancer [5]. Additionally, miRNAs can serve as

* Corresponding authors. Key Laboratory of Clinical Laboratory Diagnostics (Ministry of Education), College of Laboratory Medicine, Chongqing Medical University, Chongqing 400016, China.
*E-mail addresses:* dingshijia@163.com (S. Ding), hxju@nju.edu.cn (H. Ju).

http://dx.doi.org/10.1016/j.aca.2016.07.007
0003-2670/

biomarkers for a variety of cancers at different stages of the disease [4,6]. Therefore, methods for quantification and visualisation of aberrant miRNA expression are urgently needed for early clinical diagnosis.

Owing to their small sizes, high sequence homology among family members, and low abundance, miRNAs can be difficult to detect and quantify. Conventional analytical methods include northern blotting, polymerase chain reaction (PCR), and microarrays. However, northern blotting and microarrays are limited by time-consuming operation processes and poor sensitivity [7,8]. PCR, a widely used ultrasensitive method, is restricted by the laborious reverse transcription process and the requirement for a high-precision thermal cycler [9]. Based on these limitations, novel methods that exhibit high sensitivity, selectivity, and simplicity are needed for miRNA detection.

To explore alternative methods, extensive efforts have been made to develop a variety of biosensors for miRNA detection, including surface plasmon resonance (SPR) [10] and colorimetric [11], electrochemical [12], fluorescent [13], and chemiluminescent (CL) biosensors [14]. Among these methods, CL biosensors have attracted much attention owing to its high sensitivity, good stability, and visual detection in homogeneous solution without separation and washing steps. Additionally, to achieve sensitive sequence-specific miRNA sensing, various isothermal amplification strategies based on enzyme activity have been developed [15], including rolling circle amplification (RCA) [16–18], loop-mediated isothermal amplification (LAMP) [19], and exponential isothermal amplification reaction (EXPAR) [20–22]. Of these strategies, EXPAR is a promising, feasible, and simple technique for sensing trace amounts of nucleic acids owing to its isothermal nature, ultrahigh amplification efficiency, and rapid amplification kinetics [23].

To date, EXPAR-based biosensors, including surface-enhanced Raman spectroscopy (SERS) and electrochemical biosensors, have been widely developed for sensitive detection of miRNAs [24,25]. Moreover, EXPAR coupled with enzymatic cascades can be used as a powerful tool to develop various biosensors, such as CL biosensors for ultrasensitive detection of transcription factors and telomerase activity [26,27] or fluorescent biosensors for ultrasensitive detection of miRNAs and platelet-derived growth factor [28,29]. This combined strategy exhibits excellent amplification capability, enhanced design flexibility, and improved analytical performance. In addition, CL, as a widely used method for detection of biomarkers in clinical diagnosis, has also been shown to have potential applications in miRNA detection due to its superior features of simple instrumentation, rapid response, and low cost [30,31]. Therefore, further development of CL imaging biosensors is needed for ultrasensitive, specific, and visual detection of miRNAs by integration of cascade EXPAR strategies.

In this study, we aimed to establish an ultrasensitive and specific biosensing strategy for the detection of miRNAs using a CL imaging method based on cascade exponential isothermal amplification machinery. Hairpin probe-mediated amplification machinery enabled the biosensing platform to exhibit a low detection limit of 2.91 fM towards *miR-21* detection and ensured high selectivity using a nucleic acid switch with a stem-loop conformation. Importantly, the CL imaging method established in this study was based on a homogeneous, isothermal assay system, making the sensing platform easy to operate and providing promising alternative tools for quantification and visualisation of miRNA.

## 2. Materials and methods

### 2.1. Materials and apparatus

The high-performance liquid chromatography (HPLC)-purified oligonucleotides used in the study were synthesised by SangonInc. (Shanghai, China), and all sequences are listed in Table S1. The Klenow fragment (exo-) DNA polymerase, Nb.*Bbv*CI nicking endonuclease, and deoxyribonucleoside triphosphate (dNTP) mix were purchased from New England Biolabs Ltd. (Beijing, China). Hemin was obtained from Sigma-Aldrich (St. Louis, MO, USA), whereas dimethyl sulfoxide (DMSO) and 4-(2-hydroxyethyl) piperazine-1-ethanesulfonic acid sodium salt (HEPES) were from Sangon Inc. The stock solution of 1.0 μg $\mu L^{-1}$ total RNA extracted from breast adenocarcinoma (MCF-7) cells was obtained from Ambion (CA, USA). Hemin stock solution (10 mM) was prepared in DMSO and stored in the dark at −20 °C. The CL reagent kits were ordered from Advansta (CA, USA). All solutions were prepared and diluted in diethyprocarbonated (DEPC)-treated water. All other reagents were of analytical grade, and Millipore-Q water (S18 MΩ) was used in all experiments. An IFFM-E luminescent analyser (Remax, China) was used to record the kinetic behaviours of the CL reaction catalysed by the amplified HRP-mimicking DNAzyme. A cooled low-light CCD camera (BioImaging Systems ChemiHR 410 camera, UVP) was implemented to capture images of the CL catalysed by the generated DNAzyme. Gel electrophoresis was performed on a DYY-6C electrophoresis analyser (Liuyi Instrument Company, China) and imaged on a Bio-Rad ChemDocXRS (Bio-Rad, Hercules, CA, USA).

### 2.2. Cascade isothermal exponential amplification reaction

The cascade isothermal amplification reaction was carried out in 20 μL of total reaction solution consisting of 2.5 U Klenow fragment DNA polymerase, 5 U Nb.*Bbv*CI nicking endonuclease, 500 μM dNTPs, 20 nM template I, 30 nM template II, and different concentrations of *miR-21* (10 fM to 10 nM). First, the one-pot reaction system was incubated at 37 °C for 1.5 h in a mixed buffer of NEBuffer 2 (50 mM NaCl, 10 mM Tris-HCl, 10 mM $MgCl_2$, 1 mM DTT, pH 7.9) and CutSmart Buffer (50 mM potassium acetate, 20 mM Tris-acetate, 10 mM magnesium acetate, 100 μg·$mL^{-1}$BSA, pH 7.9). Then, the resulting mixture was heated to 80 °C for 20 min to terminate the cascade isothermal amplification reaction.

### 2.3. Chemiluminescence measurement

The CL system contained 3 μL of the above resulting solution and 27 μL HEPES solution (pH 8.6, 2 5 mM HEPES, 200 mM NaCl, 20 mM KCl, Triton X-100 [0.05%, w/v], and DMSO [1%, v/v]). Next, 0.75 μL of 4 μM hemin solution was added to the system, and the samples were incubated for 30 min at room temperature. Four microliters of CL substance was then immediately transferred to the system for CL measurement with a static method using a luminescent analyser. Similarly, three volumes of the above CL reaction solution were transferred into a well of a microplate, and the CL imaging signal was collected by a CCD camera with a 3-min dynamic integration.

### 2.4. Nondenaturing polyacrylamide gel electrophoresis (PAGE)

Native PAGE was performed on 10% acrylamide gels in 1 × TBE buffer (90 mM Tris-HCl, 90 mM boric acid, 2 mM EDTA, pH 7.9) at a constant voltage of 110 V for 35 min. The gel was then imaged using a Molecular Imager Gel Doc XR (Bio-Rad) after ethidiumbromide (EB) staining for 30 min.

## 3. Results and discussion

### 3.1. Principle of the cascade EXPAR machinery-based biosensing strategy

The principle of the cascade EXPAR machinery is illustrated in Scheme 1. Hairpin probe template I was designed with three functional regions: region I, region II, and region III. Region I incorporated a sequence to generate product I in the stem region. Region II contained a sequence complementary to the loop region of the target miRNA. Region III contained an Nb.*Bbv*CI nicking endonuclease recognition sequence (5′-CCTCAGC-3′) in the region adjacent to the stem and loop region. Additionally, linear probe template II was designed to include a region (region I) with a sequence complementary to triggers at the 5′ terminus, a region (region IV) with a sequence complementary to HRP-mimicking DNAzyme units at the 3′ terminus, and a region (region II) with two repeated nicking endonuclease recognition sites between the above two regions. Furthermore, the 3′ terminus of template II was labelled with a phosphate group in order to inhibit the nonspecific polymerisation of the probe by Klenow fragment DNA polymerase. Upon induction of the amplification machinery, the polymerisation reaction first generated double-stranded DNA in the presence of polymerase and dNTPs. Through the activity of nicking endonuclease, cleavage then occurred at the recognition sites, generating new sites to initiate the next round of replication, which displaced and released the existing synthesised primers at the cleavage site. Thus, a cyclical reaction involving the replication/nicking machinery was realised via continuous replication and cleavage. In the absence of *miR-21*, two DNA templates coexisted in the reaction buffer solution. In contrast, in the presence of *miR-21*, the autonomous replication/nicking machinery was initiated by the hybridisation of stem-loop probe template I and *miR-21*, generating product I as a trigger, which further activated the EXPAR replication/nicking machinery to yield numerous product II molecules as reporter units. The product II molecules assembled with hemin and formed the G-quadruplex HRP-mimicking DNAzyme nanostructure to catalyse the CL reaction. Upon addition of the CL substance, the CL response was generated.

### 3.2. Feasibility of the biosensing strategy

To confirm the feasibility of the developed biosensor based on the cascade EXPAR strategy, CL responses to different reaction systems were investigated (Fig. 1A and Fig. 1B). These reaction systems consisted of dNTPs, template I, and template II. In the presence of *miR-21* (100 pM), the systems that contained polymerase alone (curve a and image a) or nicking endonuclease alone (curve b and image b) showed slight CL signals after addition of hemin and CL substance, suggesting that little DNAzyme was generated to catalyse CL substance with the existence of polymerase alone or nicking endonuclease alone. The slight CL signals could be attributed to hemin. In the absence of *miR-21*, the system that contained both the polymerase and nicking endonuclease exhibited a slight increase in the CL signal (curve c and image c) due to the synthesis of small amounts of DNAzymes by the synergy of polymerase and endonuclease. However, upon addition of *miR-21* (100 pM) to the above system, the CL signal (curve d and image d) was greatly increased, indicating the synthesis of numerous DNAzymes upon the activation of replication/nicking machinery by *miR-21*. Thus, the developed biosensing system could be applied for the amplified detection of *miR-21*.

Additionally, the kinetic behaviours of the CL reaction catalysed by the generated DNAzyme were studied using a static method (Fig. S1). The results showed that the CL intensity corresponding to the CL reaction increased quickly to the maximum value and was maintained above 80% of the maximum value for 3 min, indicating that the stability of the CL signal was high.

Further, to verify whether the cascade EXPAR strategy could work as designed, native PAGE was performed (Fig. 1C). The distinct bands in lanes 1, 2, and 3 corresponded to *miR-21*, template I, and template II, respectively. The incubation of *miR-21* with template I resulted in a band (lane 4) with lower mobility due to the hybridisation between *miR-21* and template I. Further addition of polymerase and dNTPs to the mixture in lane 4 led to a band with an even lower mobility (lane 5), corresponding to the occurrence of extension by employing *miR-21* as primer and template I as scaffold. Similarly, addition of nicking endonuclease and dNTPs to the mixture in lane 4 caused the generation of a band at the same position as the band in lane 4 (lane 6), suggesting that the addition of nicking endonuclease did not cause any changes in the product. Importantly, the mixture in lane 4 plus polymerase, nicking endonuclease, and dNTPs generated a new band for product I (lane 7), demonstrating that the first replication/nicking machinery was activated to generate product I in the presence of polymerase, nicking endonuclease, dNTPs, template I, and *miR-21*. Furthermore, the mixture of template I and template II yielded two bands corresponding to template I and template II (lane 8), indicating that these two templates coexisted stably in the reaction system without *miR-21*. However, upon the addition of polymerase, nicking endonuclease, dNTPs, and *miR-21* to the mixture in lane 8 (lane 9), the band of product II was observed, implying that the EXPAR machinery was further activated in the cascade. Thus, the cascade EXPAR machinery proceeded as designed.

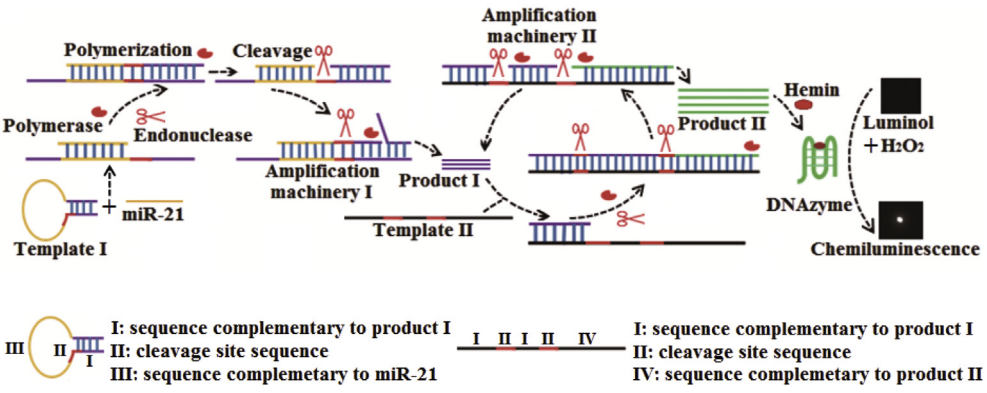


**Scheme 1.** Schematic illustration of the CL imaging strategy based on cascade EXPAR machinery for miRNA detection.

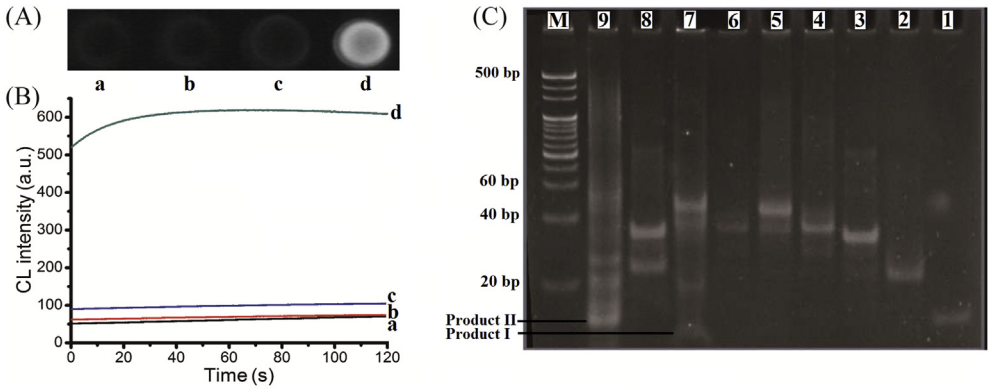


**Fig. 1.** Verification of hairpin probe-mediated cascade signal amplification. (A) CL imaging and (B) CL spectra: (a) polymerase + *miR-21*, (b) nicking endonuclease + *miR-21*, (c) polymerase + nicking endonuclease (without *miR-21*), (d) polymerase + nicking endonuclease + *miR-21*. (C) The gel electrophoresis images for cascade EXPAR products: lane 1, *miR-21*; lane 2, MB; lane 3, MG; lane 4, MB + *miR-21*; lane 5, MB + *miR-21* + polymerase; lane 6, MB + *miR-21* + nicking endonuclease; lane 7, MB + *miR-21* + polymerase + nicking endonuclease; lane 8, MB + MG; lane 9, MB + MG + *miR-21* + polymerase + nicking endonuclease; lane M, 20-bp DNA ladder.

### 3.3. Optimisation of the experimental conditions

To achieve optimal analytical performance, some experimental conditions were optimised, including the amounts of Klenow fragment DNA polymerase and Nb.*Bbv*CI nicking endonuclease, the concentration of hemin, and the molar ratios of the two DNA templates. In theory, the amplification efficiency of replication/nicking machinery mainly relies on the synergy of the polymerase and nicking enzyme. Therefore, the effects of polymerase and nicking endonuclease on the performance of the cascade exponential isothermal amplification were investigated by comparing the CL intensity ratio (S/N) of the solution with (S) and without (N) *miR-21* (100 pM). As shown in Fig. 2A and Fig. 2B, the maximum value of S/N was achieved at 2.5 U and 5 U, respectively, and these amounts were then used in subsequent experiments. The effect of the molar ratios of the two templates on the S/N value in the presence of *miR-21* was further observed by varying the molar ratios to 1:4, 2:3, 3:2, and 4:1. As shown in Fig. 3C, the S/N value increased in the range of 1:4 to 2:3 and decreased thereafter, with the optimum S/N value observed at 2:3. In addition, the S/N values of different hemin concentrations were analysed in the presence of 50 nM synthetic DNAzyme; the results showed that the optimum S/N value was achieved in the presence of 100 nM hemin (Fig. 2D).

### 3.4. Analytical performance of the biosensing strategy

To investigate the analytical performance of the developed biosensing system, we measured the CL intensities upon the addition of different concentrations of synthetic miRNA standards (10 fM to 10 nM) under optimal conditions. The results showed that

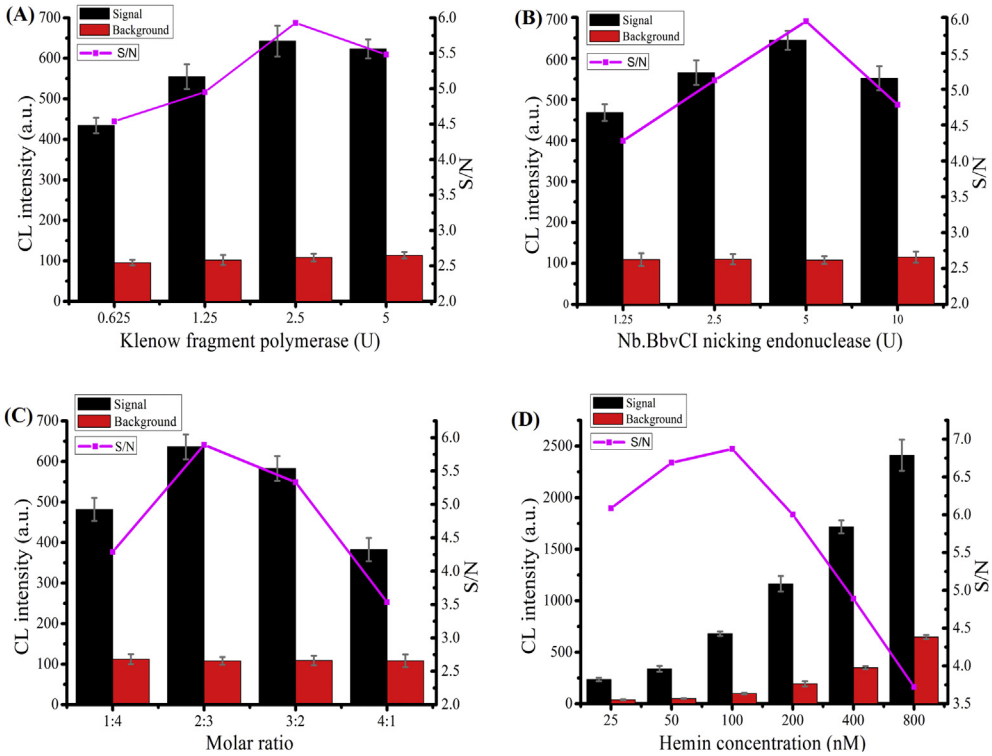


**Fig. 2.** Optimisation of the experimental conditions: (A) Klenow fragment polymerase, (B) Nb.*Bbv*CI nicking endonuclease, (C) molar ratios of template I and template II, and (D) hemin.

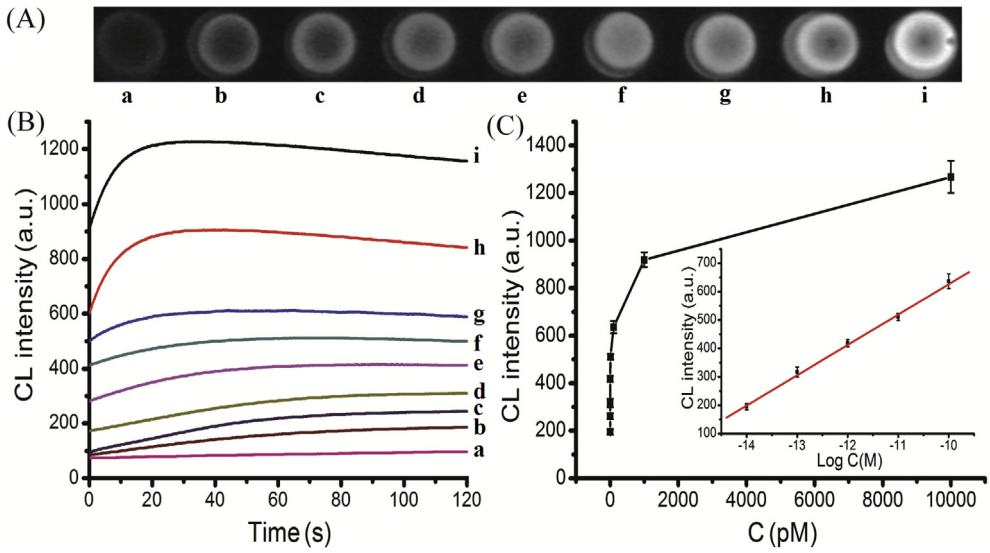


**Fig. 3.** Sensitivity of the biosensing system. (A) CL imaging upon analysis of different concentrations of *miR-21*, and (B) time-dependent CL changes upon analysis of different concentrations of *miR-21*. (a–i): 0 fM, 10 fM, 50 fM, 100 fM, 1 pM, 10 pM, 100 pM, 1 nM, and 10 nM, respectively. (C) Logarithmic plot of CL intensity versus *miR-21* concentration. Inset: linear relationship between the CL intensity and *miR-21* concentration in the range of 10 fM to 100 pM. Error bars represented the standard deviations of three independent measurements.

the CL intensity gradually increased with the increase in *miR-21* concentration from 10 fM to 10 nM, and there was a linear relationship between CL intensity and the logarithm of *miR-21* concentration in the range of 10 fM to 100 pM (Fig. 3A–C). The linear regression equation was $I = 1693.67 + 106.77\log C$ ($R^2 = 0.9978$), where I is the CL intensity, and C is the concentration of *miR-21*. The detection limit (LOD) was estimated to be 2.91 fM based on the 3σ rule. These results indicated that the increased *miR-21* activated additional cascade EXPAR machinery, resulting in the generation of DNAzymes and increased signals. In addition, the CL biosensing system was compared with other reported biosensors based on isothermal exponential amplification for nucleic acid analysis (Table S2). The results showed that the LOD of the developed method was lower than those of electrochemical biosensors [20,25], colorimetric biosensors [22], and fluorescent biosensors [32] and comparable to that of CL biosensors [30]. The achieved ultrasensitivity was attributed to cascade EXPAR and DNAzyme catalysis.

### 3.5. Selectivity of the biosensing strategy

To investigate the selectivity of the developed biosensor, different targets (100 pM) were tested, including non-complementary mismatched target (NC), double-base mismatched target (DM), single-base mismatched target (SM), and *miR-21* (Fig. 4A and B). The results showed that NC target (curve b and image b) and DM target (curve c and image c) caused negligible changes in CL signals against the blank test (curve a and image a). The SM target caused only a slight increase (curve d and image d). However, in the presence of *miR-21*, a dramatic increase in the CL signal was obtained (curve e and image e), confirming that only target *miR-21* could effectively activate the cascade EXPAR machinery to generate abundant DNAzymes for signal transduction. Thus, the designed biosensor had good selectivity and single-nucleotide difference discrimination ability, which could be attributed to the improved selectivity conferred by the hairpin probe with a stem-loop conformation [33].

### 3.6. Interference of biological samples on miRNA detection

To investigate the interference of biological samples on the CL biosensor, the proposed spiked assay was carried out by adding *miR-21* to the total RNA extracted from MCF-7 cells (Fig. 5A and Fig. 5B). The total RNA sample was first diluted to 400 ng $\mu L^{-1}$ with

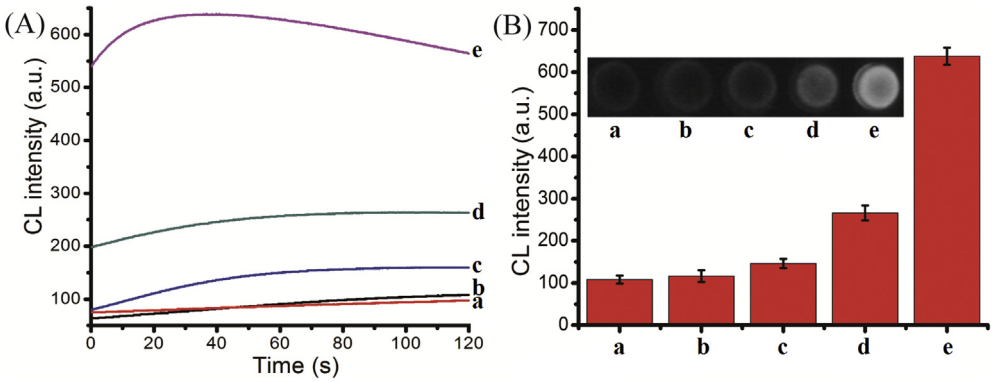


**Fig. 4.** Selectivity of the biosensing system. (A) CL spectra, (B) CL intensity, and CL images in response to (a) blank, (b) non-complementary target, (c) double-base mismatched target, (d) single-base mismatched target, and (e) *miR-21*. Error bars represent the standard deviations of three independent experiments.

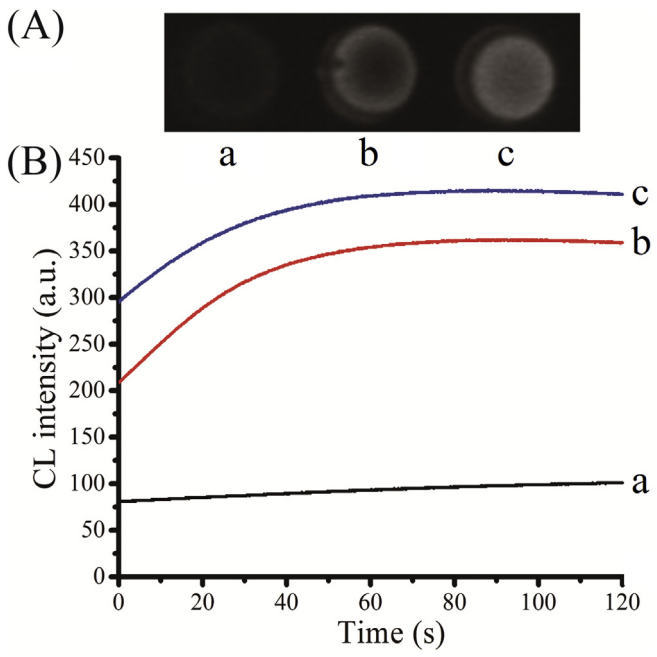


**Fig. 5.** Interference of the biological samples on miRNA detection. (A) CL images and (B) CL spectra in response to (a) blank, (b) total RNA, and (c) *miR-21* + total RNA.

DEPC-treated water, and 200 ng of the total RNA sample was then added into 20 μL of the reaction system for CL detection. According to the calibration curve (Fig. 3A), the amount of *miR-21* in 200 ng of total RNA sample was estimated to be 10.2 amol (RSD = 2.8%, n = 5), and the signal response (curve b and image b) could be distinguished from that of the blank (curve a and image a). To further investigate the interference caused by the complex matrix, 10 amol of *miR-21* was spiked into 200 ng of total RNA for measurement. The amount of *miR-21* in the spiked total RNA was estimated to be 19.8 amol (curve c and image c) with a recovery of 96.0% (RSD = 3.2%, n = 5), indicating that the analytical performance of the designed biosensor was not comprised in complex samples. These results demonstrated that the biosensing method had a high potential for miRNA detection in biological samples.

## 4. Conclusions

In summary, we established a novel CL imaging method for miRNA assays based on a hairpin probe-mediated cascade of EXPAR machinery. The biosensing strategy showed ultrasensitive detection toward target miRNA owing to the cascade of exponential isothermal amplification and DNAzyme catalysis, which mediated CL signal transduction. Additionally, the biosensing strategy achieved excellent detection selectivity resulting from the design of a hairpin probe with a stem-loop conformation. Moreover, this method was successfully applied for the detection of *miR-21*in a complex matrix. Importantly, this biosensing strategy has the advantages of isothermal, homogeneous, label-free detection without the need for sophisticated operation procedures or instruments. These features make the detection technique easy to adapt for miRNA determination [34,35]. Thus, this biosensing strategy may provide a powerful tool for miRNA detection in clinical diagnosis.

## Acknowledgements

This work was supported by the National Natural Science Foundation of China (grant nos. 21475068 and 81572080), Natural Science Foundation Project of CQ (grant no. cstc2014kjrc-qnrc10001), and Research Fund for Postgraduate Innovation Project of Chongqing (grant no. CYB14080).

## Appendix A. Supplementary data

Supplementary data related to this article can be found at http://dx.doi.org/10.1016/j.aca.2016.07.007.

## References

[1] D.P. Bartel, MicroRNAs: genomics, biogenesis, mechanism, and function, Cell 116 (2004) 281–297.
[2] A. Lujambio, S.W. Lowe, The microcosmos of cancer, Nature 482 (2012) 347–355.
[3] G.A. Calin, C.M. Croce, MicroRNA-cancer connection: the beginning of a new tale, Cancer Res. 66 (2006) 7390–7394.
[4] J. Jarry, D. Schadendorf, C. Greenwood, A. Spatz, L.C. van Kempen, The validity of circulating microRNAs in oncology: five years of challenges and contradictions, Mol. Oncol. 8 (2014) 819–829.
[5] C.J. Cheng, R. Bahal, I.A. Babar, Z. Pincus, F. Barrera, C. Liu, A. Svoronos, D.T. Braddock, P.M. Glazer, D.M. Engelman, W.M. Saltzman, F.J. Slack, MicroRNA silencing for cancer therapy targeted to the tumor microenvironment, Nature 518 (2015) 107–110.
[6] J. Wang, K.Y. Zhang, S.M. Liu, S. Sen, Tumor-associated circulating microRNAs as biomarkers of cancer, Molecules 19 (2014) 1912–1938.
[7] A. Válóczi, C. Hornyik, N. Varga, J. Burgyán, S. Kauppinen, Z. Havelda, Sensitive and specific detection of microRNAs by northern blot analysis using LNA-modified oligonucleotide probes, Nucleic Acids Res. 32 (2004) e175.
[8] I. Lee, S.S. Ajay, H. Chen, A. Maruyama, N. Wang, M.G. McInnis, B.D. Athey, Discriminating single-base difference miRNA expressions using microarray Probe Design Guru (ProDeG), Nucleic Acids Res. 36 (2008) e27.
[9] C. Chen, D.A. Ridzon, A.J. Broomer, Z. Zhou, D.H. Lee, J.T. Nguyen, M. Barbisin, N.L. Xu, V.R. Mahuvakar, M.R. Andersen, K.Q. Lao, K.J. Livak, K.J. Guegler, Real-time quantification of microRNAs by stem-loop RT-PCR, Nucleic Acids Res. 33 (2005) e179.
[10] D. Zhang, Y. Yan, W. Cheng, W. Zhang, Y. Li, H. Ju, S. Ding, Streptavidin-enhanced surface plasmon resonance biosensor for highly sensitive and specific detection of microRNA, Microchim. Acta 180 (2013) 397–403.
[11] J. Zhuang, W. Lai, G. Chen, D. Tang, A rolling circle amplification-based DNA machine for miRNA screening coupling catalytic hairpin assembly with DNAzyme formation, Chem. Commun. 50 (2014) 2935–2938.
[12] J. Zhang, D.Z. Wu, S.X. Cai, M. Chen, Y.K. Xia, F. Wu, J.H. Chen, An immobilization-free electrochemical impedance biosensor based on duplex-specific nuclease assisted target recycling for amplified detection of microRNA, Biosens. Bioelectron 15 (2016) 452–457.
[13] X. Zuo, F. Xia, Y. Xiao, K.W. Plaxco, Sensitive and selective amplified fluorescence DNA detection based on exonuclease III-aided target recycling, J. Am. Chem. Soc. 132 (2010) 1816–1818.
[14] C. Ma, E.S. Yeung, S. Qi, R. Han, Highly sensitive detection of microRNA by chemiluminescence based on enzymatic polymerization, Anal. Bioanal. Chem. 402 (2012) 2217–2220.
[15] L. Yan, J. Zhou, Y. Zheng, A.S. Gamson, B.T. Roembke, S. Nakayama, H.O. Sintim, Isothermal amplified detection of DNA and RNA, Mol. Biosyst. 10 (2014) 970–1003.
[16] S. Bi, Y. Cui, L. Li, Dumbbell probe-mediated cascade isothermal amplification: a novel strategy for label-free detection of microRNAs and its application to real sample assay, Anal. Chim. Acta 760 (2013) 69–74.
[17] Y. Cheng, X. Zhang, Z. Li, X. Jiao, Y. Wang, Y. Zhang, Highly sensitive determination of microRNA using target-primed and branched rolling-circle amplification, Angew. Chem. Int. Ed. 48 (2009) 3268–3272.
[18] F. Wang, C.H. Lu, X. Liu, L. Freage, I. Willner, Amplified and multiplexed detection of DNA using the dendritic rolling circle amplified synthesis of DNAzyme reporter units, Anal. Chem. 86 (2014) 1614–1621.
[19] C. Li, Z. Li, H. Jia, J. Yan, One-step ultrasensitive detection of microRNAs with loop-mediated isothermal amplification (LAMP), Chem. Commun. 47 (2011) 2595–2597.
[20] Y. Yu, Z. Chen, W. Jian, D. Sun, B. Zhang, X. Li, M. Yao, Ultrasensitive electrochemical detection of avian influenza A (H7N9) virus DNA based on isothermal exponential amplification coupled with hybridization chain reaction of DNAzyme nanowires, Biosens. Bioelectron. 64 (2015) 566–571.
[21] H. Jia, Z. Li, C. Liu, Y. Cheng, Ultrasensitive detection of microRNAs by exponential isothermal amplification, Angew. Chem. Int. Ed. 49 (2010) 5498–5501.
[22] J. Nie, D.W. Zhang, C. Tie, Y.L. Zhou, X.X. Zhang, G-quadruplex based two-stage isothermal exponential amplification reaction for label-free DNA colorimetric detection, Biosens. Bioelectron. 56 (2014) 237–242.
[23] J. Van Ness, L.K. Van Ness, D.J. Galas, Isothermal reactions for the amplification of oligonucleotides, Proc. Natl. Acad. Sci. U. S. A. 100 (2003) 4504–4509.
[24] L.P. Ye, J. Hu, L. Liang, C.Y. Zhang, Surface-enhanced Raman spectroscopy for simultaneous sensitive detection of multiple microRNAs in lung cancer cells, Chem. Commun. 50 (2014) 11883–11886.

[25] Y. Yu, Z. Chen, L. Shi, F. Yang, J. Pan, B. Zhang, D. Sun, Ultrasensitive electrochemical detection of microRNA based on an arched probe mediated isothermal exponential amplification, Anal. Chem. 86 (2014) 8200–8205.
[26] F. Ma, Y. Yang, C.Y. Zhang, Ultrasensitive detection of transcription factors using transcription-mediated isothermally exponential amplification induced chemiluminescence, Anal. Chem. 86 (2014) 6006–6011.
[27] L.J. Wang, Y. Zhang, C.Y. Zhang, Ultrasensitive detection of telomerase activity at the single-cell level, Anal. Chem. 85 (2013) 11509–11517.
[28] Y. Zhang, C.Y. Zhang, Sensitive detection of microRNA with isothermal amplification and a single-quantum-dot-based nanosensor, Anal. Chem. 84 (2012) 224–231.
[29] Z.Z. Zhang, C.Y. Zhang, Highly sensitive detection of protein with aptamer-based target-triggering two-stage amplification, Anal. Chem. 84 (2012) 1623–1629.
[30] S. Bi, J. Ye, Y. Dong, H. Li, W. Cao, Target-triggered cascade recycling amplification for label-free detection of microRNA and molecular logic operations, Chem. Commun. 52 (2016) 402–405.
[31] Z. Yang, Y. Cao, J. Li, J. Wang, D. Du, X. Hu, Y. Lin, A new label-free strategy for a highly efficient chemiluminescence immunoassay, Chem. Commun. 51 (2015) 14443–14446.
[32] J. Xu, Z.S. Wu, W. Shen, H. Xu, H. Li, L. Jia, Cascade DNA nanomachine and exponential amplification biosensing, Biosens. Bioelectron. 73 (2015) 19–25.
[33] K. Wang, Z. Tang, C.J. Yang, Y. Kim, X. Fang, W. Li, Y. Wu, C.D. Medley, Z. Cao, J. Li, P. Colon, H. Lin, W. Tan, Molecular engineering of DNA: molecular beacons, Angew. Chem. Int. Ed. 48 (2009) 856–870.
[34] B.T. Roembke, S. Nakayama, H.O. Sintim, Nucleic acid detection using G-quadruplex amplification methodologies, Methods 64 (2013) 185–198.
[35] Y. Zhao, F. Chen, Q. Li, L. Wang, C. Fan, Isothermal amplification of nucleic acids, Chem. Rev. 115 (2015) 12491–12545.